DRA-7a. CHEMISTRY AND MINERALOGY WITH CHANGE IN PARTICLE SIZE

V. T. McLemore, November 30, 2008, revised April 14, 2009 (reviewed by A. Campbell, G. Robinson)

1. STATEMENT OF THE PROBLEM

What are the differences in geochemistry, mineralogy, and acid-base accounting (ABA) between different particle size fractions? Understanding the distribution of minerals and geochemistry with different particle size fractions is important for understanding mobility and availability of minerals to dissolution and oxidation during weathering.

2. PREVIOUS WORK

Weathering of minerals involves mostly surface reactions and the rates of these reactions depend upon the available reactive surface area of the mineral. Mineral surface area is dependent on the mineralogy, the extent to which the mineral is liberated from the rock matrix, particle size (especially mineral grain size), and the surface morphology (i.e. roughness of the mineral surface; Lapakko et al., 1998; Lapakko, 2003). Furthermore, when mineral surfaces are covered with coatings, such as Fe oxyhydroxides, oxidation and dissolution of the mineral can be inhibited. Thus, particles of different sizes expose different proportions of the surfaces for chemical reaction, which plays an important role in weathering.

Many studies have examined the variations in composition between different particle size fractions. Strömberg and Banwart (1999) showed large differences in weathering rates between fine waste rock material and larger particles (diameters >0.25 mm) and found that waste rock with diameters less than 0.25 mm (27% of the total mass) accounts for 80% of both the sulfide and silicate weathering. Taboada et al. (2006) showed that Zr and Ti behave differently in residual weathering soil profiles; Zr is enriched in the silt fraction, whereas Ti is enriched in the silt and clay fractions and depleted in the sand fraction. Dultz (2002) cautions that normally feldspars are found in the coarser fractions of soils, but breakdown of feldspar grains by physical weathering could increase the surface area and therefore, increase the reactivity of the grains to weathering. Dultz (2002) also cautions that the parent material affects the weathering of feldspars. Brandvold and McLemore (1998) and McLemore et al. (1995) found that the smallest size fractions (<63 μm) of stream sediments contained the largest concentrations of metals (Cu, Pb, Zn) in the Pecos and La Bajada Rivers in northern New Mexico. Dinelli et al. (2007) found that the effects of grain-size distribution on mineralogy and geochemistry are greater in sediments that have not undergone diagenesis, compaction, or lithification. Some chemical indices are not affected by grain size distribution, including Ni/Al, Cr/Al, and Mg/Al and other indices are affected only by the coarse fraction, including SiO2/Al2O3, Na/Al, Zr/Rb, Zr/V, Y/Rb, Y/V, and Ti/V (Dinelli et al (2007).

3. TECHNICAL APPROACH

Samples were collected in the field and analyzed in the laboratory, similar to other samples in the QRPWASP (see DRA-0, project SOPs). The laboratory methods included X-ray fluorescence whole-rock geochemistry (SOP 28), petrographic analysis (SOP 24), clay mineralogical analyses by X-ray diffraction (SOP 29), paste pH and conductivity (SOP 11), particle size analysis (SOP 33), Acid Base Accounting (ABA; SOP 62) and Net Acid Generation (NAG; SOP 52) and quantitative mineralogy determination (DRA-5; McLemore et al., 2009). The procedures used for the laboratory methods are presented in project SOPs. Table 1 lists the samples collected from each location and the different particle size fractions used for the study and Figures 1 and 2 are location maps. Samples were selected 1) to cover a range in weathering intensities, 2) to include rock-pile and analog materials, and 3) on availability of enough of the sample to perform the analysis. However, not enough material was available for the SPR sample for the five different particle size fractions and only four fractions were obtained. Graf (2008) also examined the variations in mineralogy and chemistry with different particle size fractions in the Hansen alteration scar.

TABLE 1. Samples used for the particle size fraction study. The geologic unit for samples from GHN is in parenthesis and described in more detail in McLemore et al. (2008a). Locations of samples are in Figures 1 and 2.

Location	Samples	Number of Size Fraction	Size Fractions (inches)
Goathill North (GHN) rock pile	GHN-JRM-0001 (J) GHN-JRM-0002 (N) GHN-KMD-0088 (O)	5	0.75, 0.5, 0.187, 0.0787, <0.0787
Goat Hill Debris Flow	MIN-AAF-0001 MIN-AAF-0004 MIN-SAN-0002	5	1, 0.75, 0.5, 0.187, 0.0787
Questa Pit Alteration Scar	QPS-AAF-0001 QPS-AAF-0003 QPS-AAF-0005 QPS-AAF-0009 QPS-SAN-0002	5	1, 0.75, 0.5, 0.187, 0.0787
Spring Gulch (SPR) rock pile	SPR-SAN-0002	4	0.75, 0.5, 0.187, 0.0787

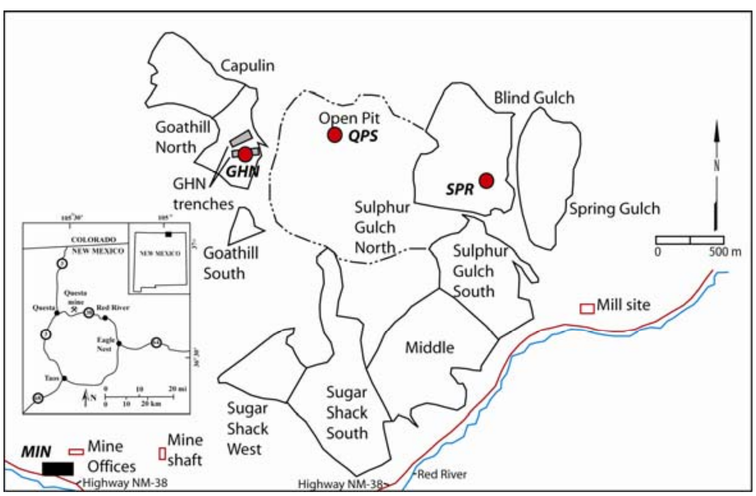

FIGURE 1. Questa rock piles and other mine features, including approximate locations of samples used for particle size analysis.

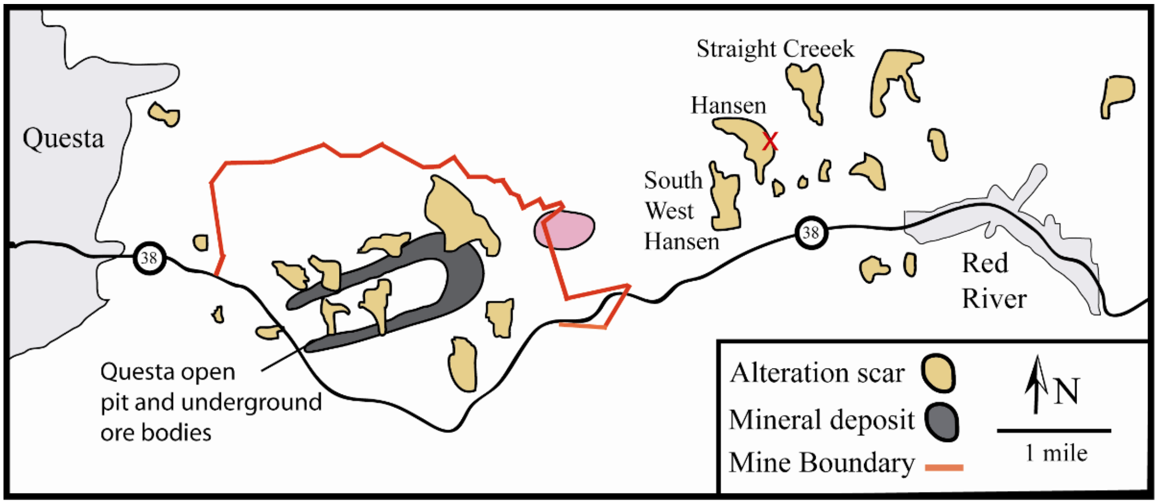

FIGURE 2. Location of alteration scars in the Red River valley, including the approximate location of the samples for particle size analysis from Hansen alteration scar (HAS samples, Graf, 2008).

4. CONCEPTUAL MODEL

Variations in mineral and particle sizes in the Questa rock piles are a result of several processes:

- Original primary igneous crystallization results in minerals of different sizes in a fine-grained groundmass that can be subsequently liberated from the rock fragments (McLemore et al., 2008b; DRA-1)
- Pre-mining hydrothermal alteration, especially replacement of primary silicate minerals by hydrothermal clay minerals (Molling, 1968; Graf, 2008; McLemore et al., 2008b; DRA-1)
- Regional fracturing of the pre-mined rock during igneous intrusion and hydrothermal alteration (Caine, 2003, 2006; Ludington et al., 2005)
- Breaking up of the rock material during blasting, hauling, and dumping during mining (URS Corporation, 2003; McLemore et al., 2008a)
- Physical (freeze-thaw) and chemical weathering (Ludington et al., 2005; Graf, 2008; DRA-27)
- Precipitation of weathered minerals, such as gypsum, along fractures and veins, which increase the mineral volume and break apart the rock (DRA-25).
- Erosion.

5. STATUS OF COMPONENT INVESTIGATION

For some samples, paste pH values decreases from the coarse-size fraction to the fine-size fraction, but not all samples show a large decrease (Fig. 3, Appendix 1, Table 1-1). The neutralizing potential (NP) is higher in the coarse-size fractions than the fine-size fractions (Appendix 1, Table 1-2). The net acid producing potential (NAPP) of the coarse-size fractions (<0.0787 inch) is significantly lower than that of the fine-size fractions (>0.0787 inch; Table 1-2). The coarse-size fractions are less acid generating than fine-size fractions.

Mineral and chemical composition of the different size fractions are in Appendix 1 (Tables 1-3, 1-4). Feldspar and pyrite generally increases in the coarse-size fraction (Fig.

4). Total clay minerals and gypsum + jarosite decrease in the coarse-size fraction (Fig. 4). In some samples, calcite increases in the coarse-size fraction, but some samples show no variations with different particle size fractions (Fig. 4). Na_2O and S increase in the coarse-size fraction, whereas SO_4 decreases in the coarse-size fraction (Fig. 5). Al_2O_3 concentration changes little between the different size fractions. Figure 6 shows that for most samples the larger particle size fractions are less acid generating than finer particle size fractions. Additional graphs and data are in Morkeh (2009).

Graf (2008) found an increase in FeO, CaO, and SO_4 between the coarse- and fine-size fractions in samples from the Hansen alteration scar. He attributes the increase in CaO and SO_4 to the precipitation of gypsum. Silicate dissolution can be recognized from coarse- to fine-size particles, as indicated by the decrease in Na_2O and K_2O, and the large change in total feldspar from coarse- to fine-size fractions. The clay mineralogy was consistent between the coarse- and fine-size fractions in these samples.

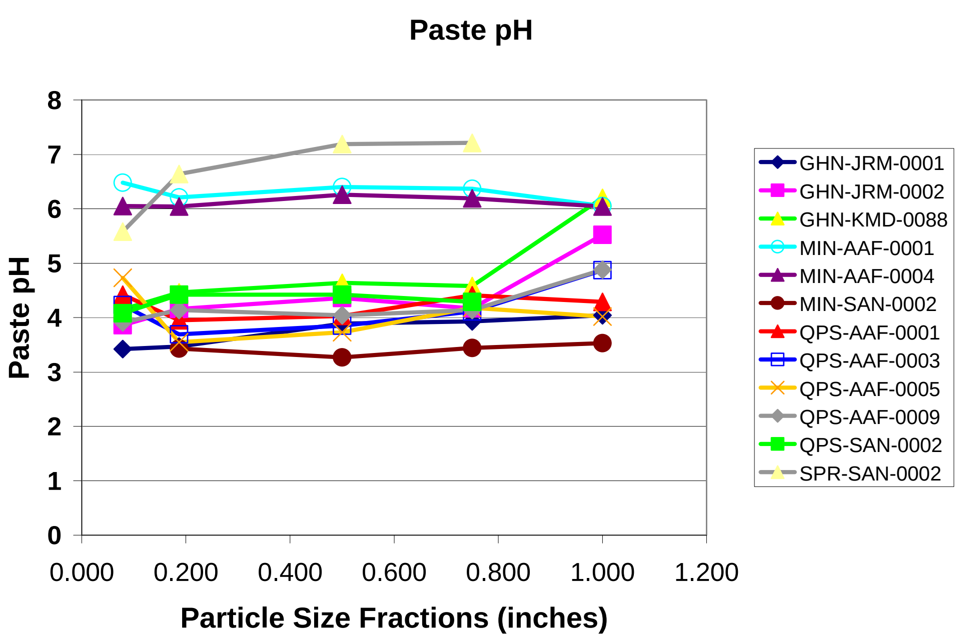

FIGURE 3. Variations of paste pH with different particle size fractions. Generally the fine-size fractions have lower paste pH values.

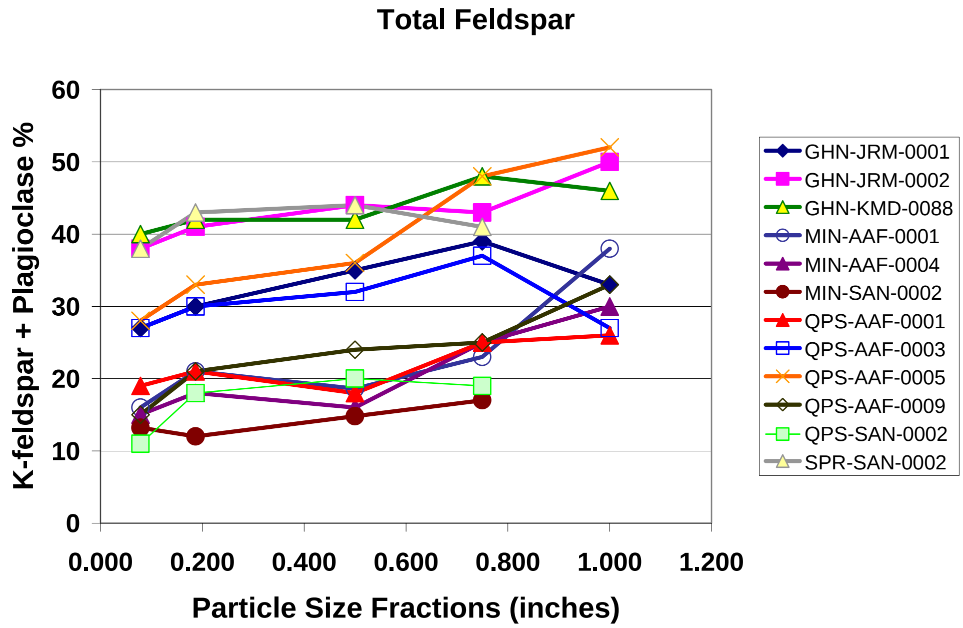

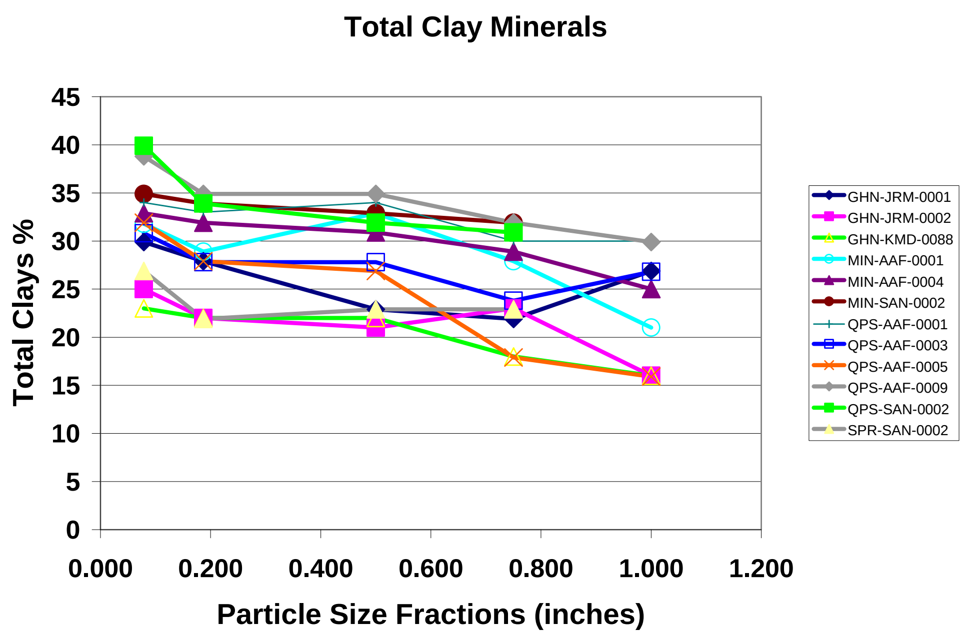

FIGURE 4. Variations in total feldspar, clay minerals, pyrite, calcite and sulfate minerals with different size fractions.

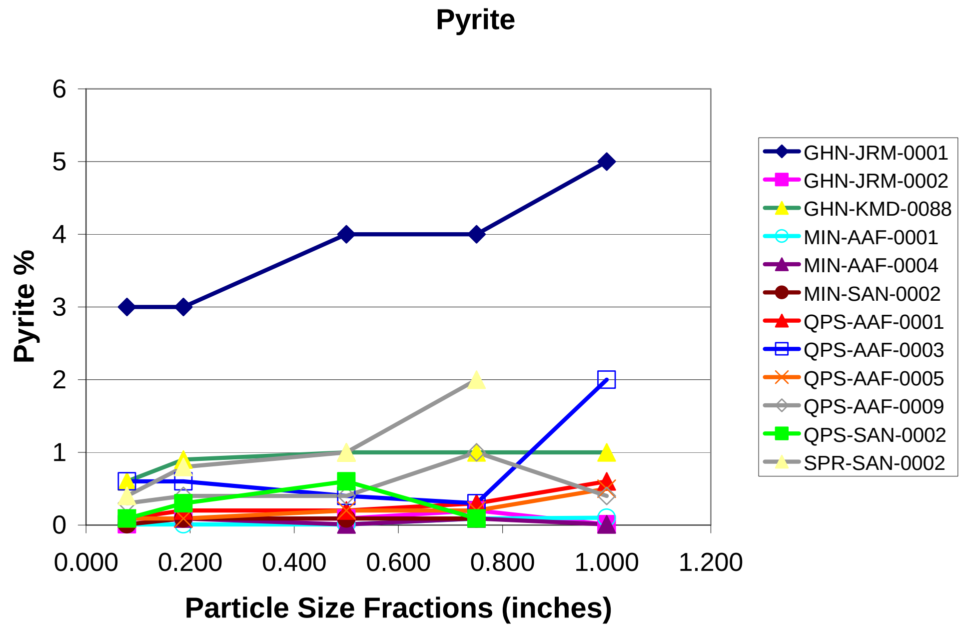

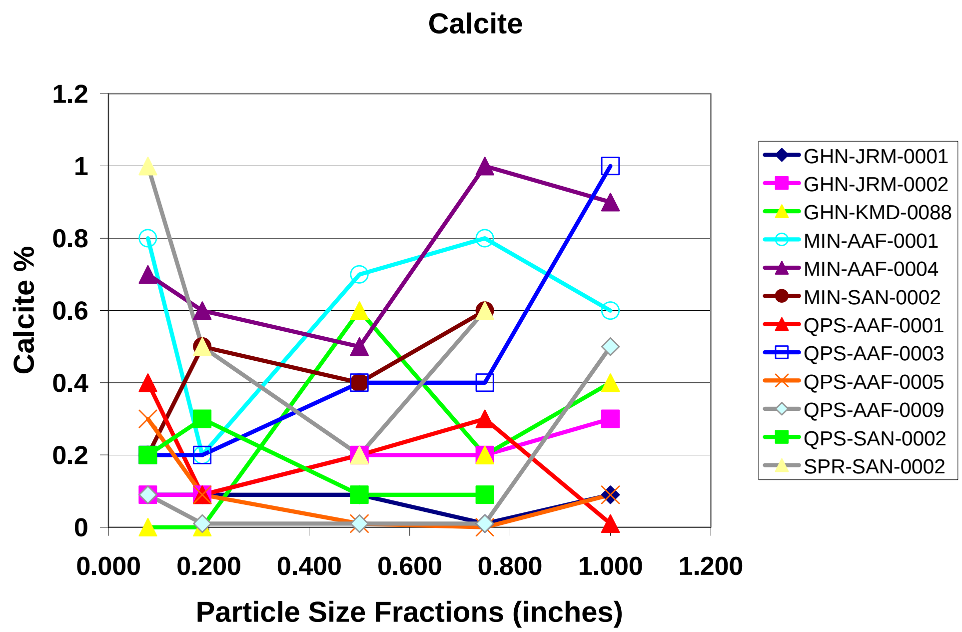

FIGURE 4 continued. Variations in total feldspar, clay minerals, pyrite, calcite and sulfate minerals with different size fractions.

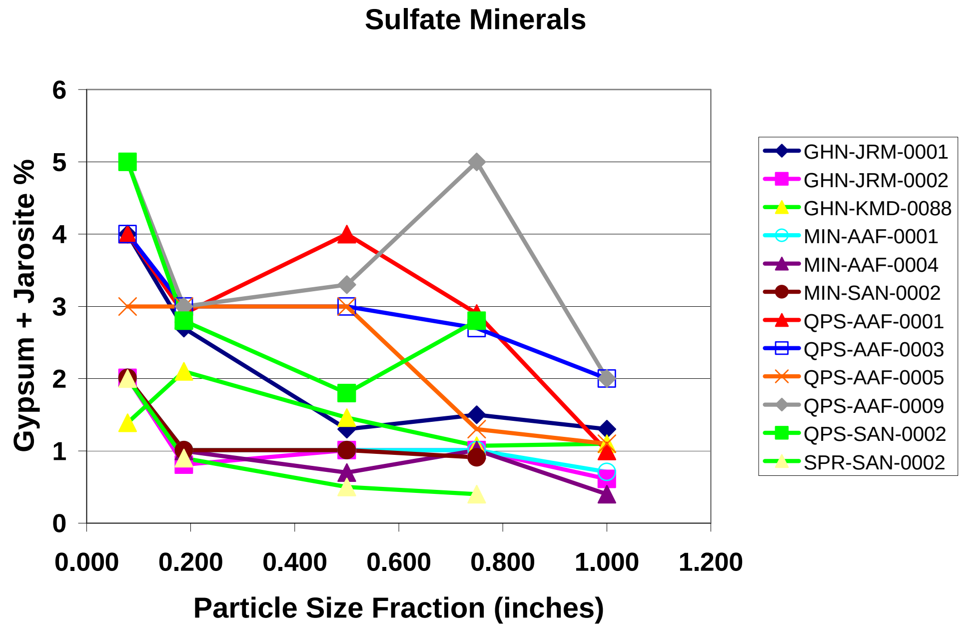

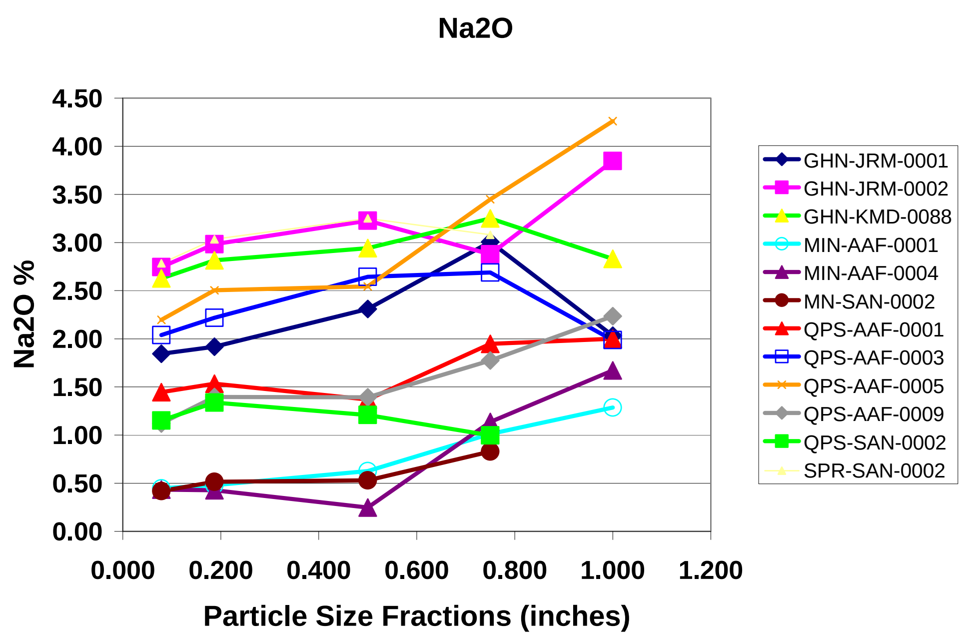

FIGURE 4 continued. Variations in total feldspar, clay minerals, pyrite, calcite and sulfate minerals with different size fractions.

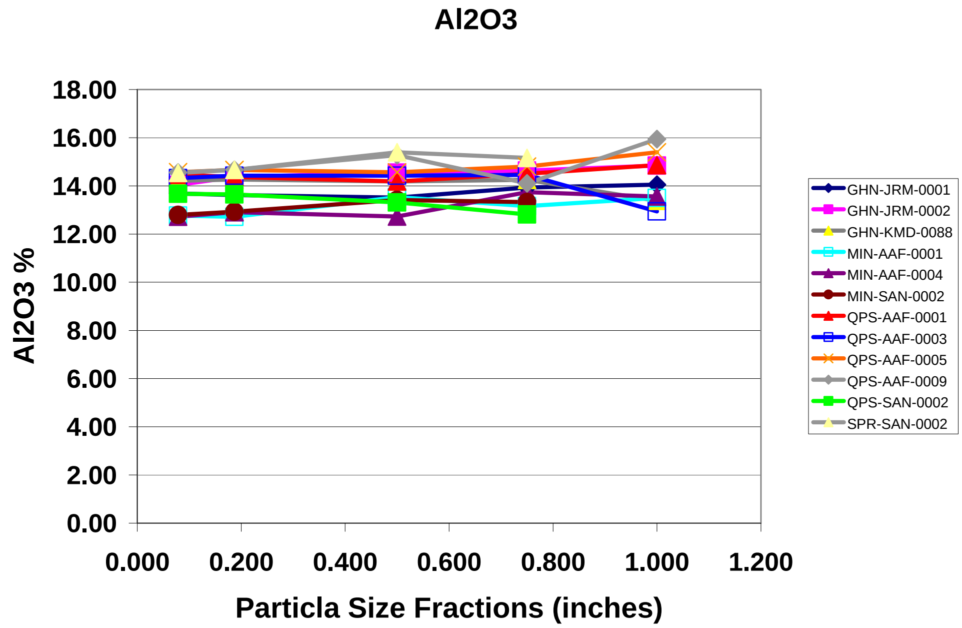

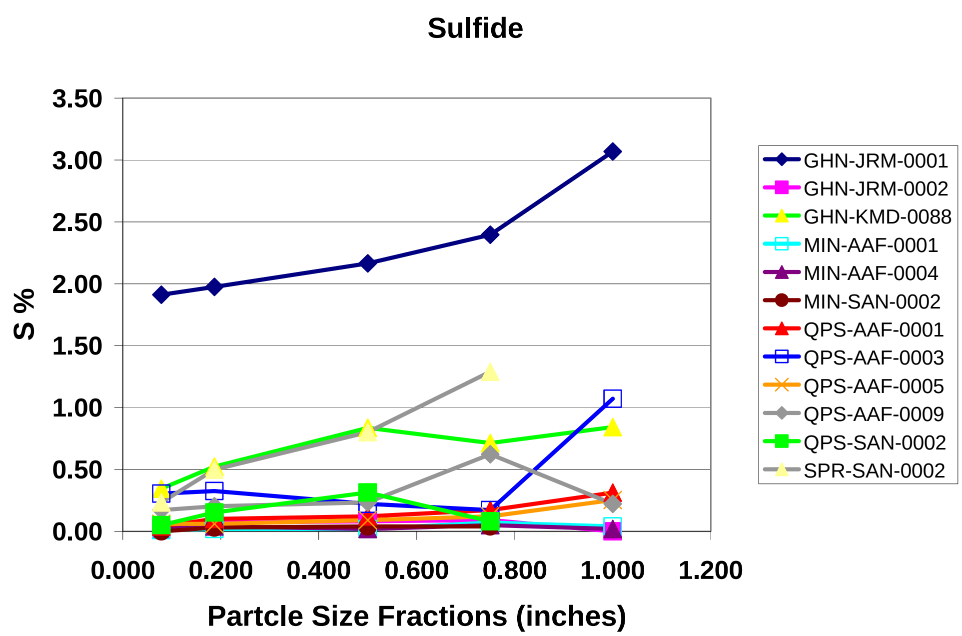

FIGURE 5. Variations in Na_2O, Al_2O_3, S and SO_4 minerals with different size fractions.

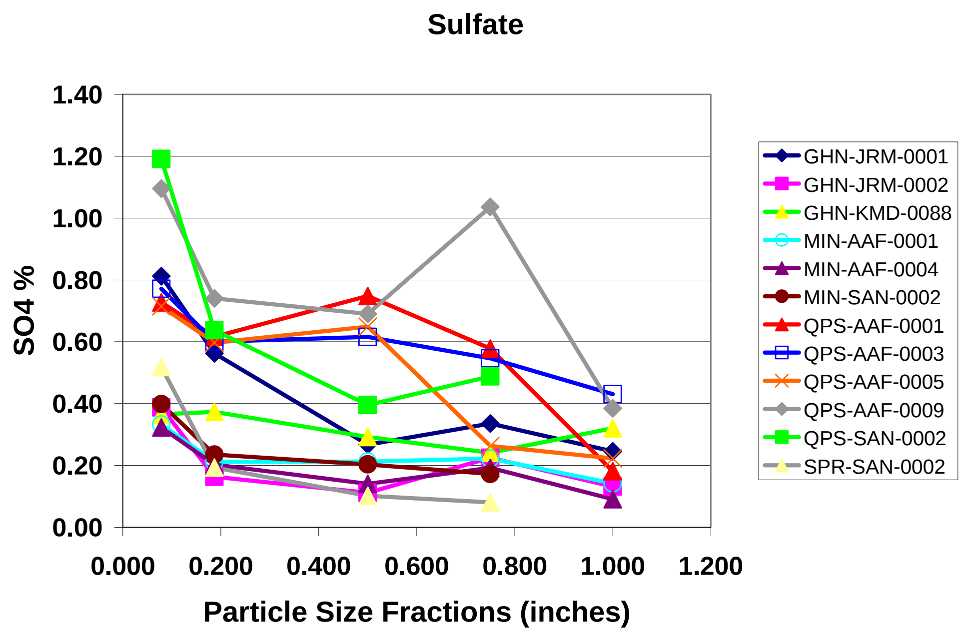

FIGURE 5 continued. Variations in Na_2O, Al_2O_3, S and SO_4 minerals with different size fractions.

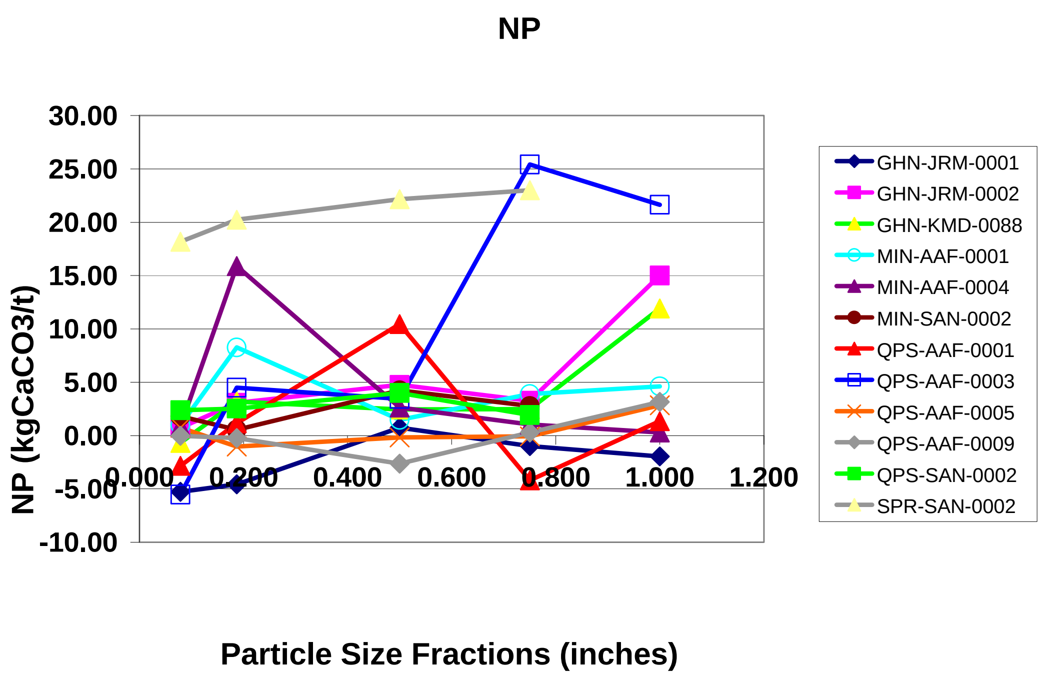

FIGURE 6. Plot of neutralizing potential distribution vs. size fraction.

6. RELIABILITY ANALYSIS

Only 12 samples were examined for differences in composition with different particle size fractions. Samples collected are complete, comparable, and representative of the lithologies and weathering intensities found at the Questa mine. Precision and accuracy are measured differently for each field and laboratory analysis (parameter), and are explained in the project reports, SOPs and DRAs (DRA-0). Most laboratory analyses depend upon certified reference standards and duplicate and triplicate analyses as defined in the project SOPs.

The sampling and analysis plans for each segment of the field program and the control of accuracy and precision as defined in the SOPs, provides a large high-quality set of observations and measurements that are adequate to support the interpretations and conclusions of this DRA.

The chemical analyses are accurate to within ±5% as determined by duplicate and triplicate analyses and comparison to known internal standards. The mineralogical analyses are estimated to be accurate to within ±10% of the reported value and compare well with other mineralogical techniques (McLemore et al., 2009; DRA 5). See McLemore and Frey (2008) for more details on the quality control and quality assurance precision and accuracy data. The quantitative mineralogical method obtained by the modified ModAn method is a reliable method that is consistent with the petrographic observations, electron microprobe analysis, clay mineral analysis, and the whole-rock chemistry of the sample and provides a method that reduces the variability that can be obtained by petrographic analysis by different petrographers (McLemore et al., 2009; DRA-5). The quantitative mineralogy obtained by this method provides a more reliable mineral composition for this project because it does quantify specific clay and sulfate minerals, which are important for understanding the rock and mineral weathering of the Questa materials.

7. CONCLUSION OF THE COMPONENT

For some samples, paste pH values decreases from the coarse-size fraction to the fine-size fraction, but not all samples show a large decrease. The coarse-size fractions are less acid generating than fine-size fractions. Feldspar and pyrite generally increase in the coarse-size fraction. Total clay minerals and gypsum + jarosite decrease in the coarse-size fraction. In some samples, calcite increases in the coarse-size fraction, but some samples show no variations in calcite with different particle size fractions. Na_2O and S increase in the coarse-size fraction, whereas SO_4 decreases in the coarse-size fraction (Fig. 5). Al_2O_3 shows little change with different size fractions. Silicate dissolution can be recognized from coarse- to fine-size particles, as indicated by the decrease in feldspar, Na_2O and K_2O from coarse- to fine-size fractions. Similar trends were found by Graf (2008) in the Hansen alteration scar. Collectively, these results are consistent with weathering being more pronounced in the fine-size fraction than the coarse-size fraction. The dissolution of pyrite, calcite, and to a lesser extent some combination of chlorite, illite, feldspars, smectite, and other silicate minerals are the predominant chemical reactions that results in the precipitation of gypsum, jarosite, soluble efflorescent salts, and Fe oxide/hydroxide minerals, mostly in the fine-size fractions, although some authigenic gypsum crystals can be quite large.

8. REFERENCES

Brandvold, L.A. and McLemore, V.T., 1998, A study of the analytical variation of sampling and analysis of stream-sediments from areas contaminated by mining and milling: Journal of Geochemical Exploration, v. 64, p. 185-196.

Caine, J.S., 2003, Questa Baseline and Pre-Mining Ground-Water Quality Investigation. 6. Preliminary Brittle Structural Geologic Data, Questa Mining District, southern Sangre de Cristo Mountains, New Mexico. U.S. Geological Survey Open-File Report 03-280, http://pubs.usgs.gov/sir/2005/5149/, accessed 11/8/08.

Caine, J.S., 2006, Questa Baseline and Pre-Mining Ground-Water Quality Investigation. 18. Characterization of brittle structures in the Questa caldera and speculation on their potential impacts on the bedrock ground-water flow system, Red River watershed, New Mexico. U.S. Geological Survey Professional Paper 1729, 37 p., http://pubs.usgs.gov/of/2003/ofr-03-280/, accessed 11/8/08.

Dinelli, E., Tateo, F., and Summa, V., 2007, Geochemical and mineralogical proxies for grain size in mudstones and siltstones from the Pleistocene and Holocene of the Po alluvial plain, Italy; in Aiibas, J., Critelli, S., and Johnson, M.J., eds., Sedimentary province and petrogenesis: Perspectives from petrography and geochemistry: Geological Society of America; Special Paper 420, p. 25-36.

Dultz, S., 2002, Effects of parent material and weathering on feldspar content in different particle size fractions from forest soils in NW Germany: Geoderma, v. 106, p. 63-81.

Graf, G.J., 2008, Mineralogical and geochemical changes associated with sulfide and silicate weathering, natural alteration scars, Taos County, New Mexico: M. S. thesis, New Mexico Institute of Mining and Technology, Socorro, 193 p., http://geoinfo.nmt.edu/staff/mclemore/Molycorppapers.htm, accessed April 28, 2008.

Lapakko, K., 2003, Solid phase characterization for metal mine waste drainage quality prediction: Preprint 03-093, 8 p.

Lapakko, K.A., Haub, J., and Antonson, D.A., 1998, Effect of dissolution time and particle size on kinetic test results: Society for Mining, Metallurgy, and Exploration, SME, Littleton, CO, preprint 98-114.

Ludington, S., Plumlee, G.S., Caine, J.S., Bove, D., Holloway, J.M., and Livo, K.E., 2005, Questa Baseline and Pre-Mining Ground-Water Quality Investigation. 10. Geologic influences on ground and surface waters in the lower Red River watershed, New Mexico. U.S. Geological Survey Scientific Investigations Report 2004-5245, http://pubs.usgs.gov/sir/2004/5245/, accessed 11/8/08.

McLemore, V.T., Ayakwah, G., Boakye, K., Campbell, A., Donahue, K., Dunbar, N., Gutierrez, L. Heizler, L., Lynn, R., Lueth, V., Osantowski, E., Phillips, E., Shannon, H., Smith, M. Tachie-Menson, S., van Dam, R., Viterbo, V.C., Walsh, P., and Wilson, G.W., 2008a, Characterization of Goathill North Rock Pile: revised unpublished report to Molycorp, Tasks: 1.3.3, 1.3.4, 1.4.2, 1.4.3, 1.11.1.3, 1.11.1.4, 1.11.2.3, B1.1.1, B1.3.2.

McLemore, V.T., Brandvold, L.A., Hossain, A.M., Pease, T.C., 1995, The effect of particle size distribution on the geochemistry of stream sediments from the upper Pecos River, San Miguel County, New Mexico: New Mexico Geological Society, Guidebook 46, p. 323–329.

McLemore, V.T., Donahue, K., and Sweeney, D., 2008b, Lithologic atlas for the Questa mine, Taos County, New Mexico: revised unpublished report to Molycorp (revised from appendix 2.3, May 2005 report).

McLemore, V.T. and Frey, B., 2008, Quality control and quality assurance report: unpublished report to Chevron, Task B1.

McLemore, V., Sweeney, D., Dunbar, N., Heizler, L. and Phillips, E., 2009, Determining quantitative mineralogy using a combination of petrographic techniques, whole rock chemistry, and MODAN: Society of Mining, Metallurgy and Exploration Annual Convention, preprint 09-20, 19 p.

Molling, P.A., 1989, Applications of the reaction progress variable to hydrothermal alteration associated with the deposition of the Questa molybdenite deposit, NM: PhD dissertation, Johns Hopkins University, 227 p.

Morkeh, J., 2009, Geochemistry and mineralogy of mine rock pile materials and different grain size fractions from the Chevron Questa mine, Taos County, New Mexico: M. S. thesis, New Mexico Institute of Mining and Technology, Socorro, in progress.

Strömberg, B. and Banwart, S.A., 1999, Experimental study of acidity-consuming processes in mining waste rock: some influences of mineralogy and particle size: Applied Geochemistry, v. 14, p. 1-16.

Taboada, T., Cortizas, A.M., García, C., García-Rodeja, E., 2006, Particle-size fractionation of titanium and zirconium during weathering and pedogenesis of granitic rocks in NW Spain: Geroderma, v. 131, p. 218-236.

URS Corporation, 2003, Mine rock pile erosion and stability evaluations, Questa mine: unpublished Report to Molycorp, Inc., 4 volumes.

9. TECHNICAL APPENDICES

APPENDIX 1. Data tables.

TABLE 1-1. Summary of paste pH and paste conductivity results of different particle size fractions.

Sample	Size Fraction (inches)	Paste pH	Paste Conductivity(mS/cm)
GHN-JRM-0001	1.000	4.04	1.86
	0.750	3.93	2.25
	0.500	3.89	2.19
	0.187	3.47	1.89
	0.079	3.42	3.21
	<0.0787	2.43	4.8
GHN-JRM-0002	1.000	5.52	1.37
	0.750	4.17	1.88
	0.500	4.36	0.7
	0.187	4.16	1.23
	0.079	3.86	2.28
	<0.0787	2.57	3.3
GHN-KMD-0088	1.000	6.2	2.55
	0.750	4.58	2.47

Sample	Size Fraction (inches)	Paste pH	Paste Conductivity(mS/cm)
	0.500	4.64	2.7
	0.187	4.46	2.68
	0.079	4.15	1.72
	<0.0787	2.83	4.32
MIN-AAF-0001	1.000	6.05	0.19
	0.750	6.37	0.25
	0.500	6.4	0.2
	0.187	6.21	0.29
	0.079	6.48	0.22
MIN-AAF-0004	1.000	6.04	0.17
	0.750	6.19	0.3
	0.500	6.26	0.19
	0.187	6.04	0.19
	0.079	6.05	0.19
MIN-SAN-0002	1.000	3.53	0.16
	0.750	3.44	0.24
	0.500	3.27	0.24
	0.187	3.43	0.23
	0.079		
QPS-AAF-0001	1.000	4.29	0.92
	0.750	4.41	1.81
	0.500	4.03	1.68
	0.187	3.95	1.68
	0.079	4.42	1.85
QPS-AAF-0003	1.000	4.87	2
	0.750	4.11	2.02
	0.500	3.85	1.76
	0.187	3.69	1.6
	0.079	4.23	1.84
QPS-AAF-0005	1.000	4.02	1.31
	0.750	4.18	1.7
	0.500	3.73	2.28
	0.187	3.55	1.61
	0.079	4.73	2.22
QPS-AAF-0009	1.000	4.88	2.08
	0.750	4.14	1.98
	0.500	4.04	2.24
	0.187	4.14	1.81
	0.079	3.91	1.93
QPS-SAN-0002	1.000		
	0.750	4.29	
	0.500	4.42	
	0.187	4.42	
	0.079	4.08	
SPR-SAN-0002	1.000		
	0.750	7.21	

Sample	Size Fraction (inches)	Paste pH	Paste Conductivity(mS/cm)
	0.500	7.19	
	0.187	6.64	
	0.079	5.58	

TABLE 1-2. Summary of ABA results of different particle size fractions.

Sample	AP (Kg CaCO3/ton)				
	1.0-0.75 inch	0.75-0.5 inch	0.5-0.187 inch	0.187-0.0787 inch	0.0787inch
GHN-JRM-0001	97.81	75.94	68.44	62.50	60.31
GHN-JRM-0002	0	2.81	2.50	2.19	0.63
GHN-KMD-0088	26.25	22.19	25.94	16.25	10.63
MIN-AAF-0001	1.25	2.19	0.63	0.63	0.31
MIN-AAF-0004	0.63	1.56	0.63	1.25	1.25
MIN-SAN-0002	na	1.25	1.25	0.94	0
QPS-AAF-0001	9.69	5.31	3.75	3.13	1.25
QPS-AAF-0003	33.44	5.31	6.88	10	9.38
QPS-AAF-0005	7.81	3.75	2.81	1.88	1.88
QPS-AAF-0009	6.88	19.38	7.19	6.25	5.31
QPS-SAN-0002	na	2.50	9.69	4.69	1.56
SPR-SAN-0002	na	40	24.69	15.31	7.19
	NP (Kg CaCO3/ton)				
	1.0-0.75 inch	0.75-0.5 inch	0.5-0.187 inch	0.187-0.0787 inch	0.0787inch
GHN-JRM-0001	-1.95	-0.99	0.74	-4.58	-5.27
GHN-JRM-0002	15.01	3.27	4.75	3.07	0.72
GHN-KMD-0088	11.91	2.47	2.45	3.19	-0.69
MIN-AAF-0001	4.61	3.89	1.46	8.26	0.98
MIN-AAF-0004	0.29	1.03	2.64	15.89	0.84
MIN-SAN-0002	na	2.77	4.23	0.55	1.79
QPS-AAF-0001	1.35	-4.19	10.45	1.16	-2.85
QPS-AAF-0003	21.64	25.42	3.44	4.49	-5.53
QPS-AAF-0005	2.85	-0.08	-0.18	-1.03	0.73
QPS-AAF-0009	3.15	0.28	-2.64	-0.24	-0.03
QPS-SAN-0002	na	1.92	3.98	2.52	2.37
SPR-SAN-0002	na	23	22.16	20.24	18.17

na – size fraction not collected

TABLE 1-3. Chemical composition of samples and different particle size fractions. Major element oxides, S, SO4, and LOI are in weight percent. Trace elements are in parts per million. Total iron is calculated as FeOT.

Sample	Size Fraction (inch)	SiO_2	TiO_2	Al_2O_3	FeOT	MnO	MgO	CaO	Na_2O	K_2O	P_2O_5
GHN-JRM-0001	whole rock	61.6	0.53	13.65	4.760	0.08	1.28	0.98	1.87	3.91	0.19
GHN-JRM-0001-56	1.000	66.2	0.54	14.33	4.425	0.07	0.99	0.41	2.03	4.18	0.20
GHN-JRM-0001-57	0.750	65.9	0.50	14.12	4.514	0.07	1.19	0.43	3.01	3.58	0.21
GHN-JRM-0001-58	0.500	67.1	0.48	13.67	4.258	0.08	1.19	0.47	2.31	3.98	0.18
GHN-JRM-0001-61	0.187	65.5	0.50	13.79	4.201	0.07	1.15	0.55	1.92	4.24	0.14
GHN-JRM-0001-62	0.079	63.6	0.53	13.82	4.331	0.08	1.21	0.82	1.84	4.06	0.16
GHN-JRM-0002	whole rock	61.0	0.84	14.36	6.896	0.36	2.57	1.72	2.82	3.33	0.40
GHN-JRM-0002-56	1.000	62.8	0.78	14.61	4.963	0.22	2.46	1.89	3.85	3.40	0.35
GHN-JRM-0002-57	0.750	61.9	0.83	14.33	5.137	0.21	2.53	1.53	2.88	3.88	0.33
GHN-JRM-0002-58	0.500	62.0	0.85	14.29	5.743	0.26	2.52	1.37	3.23	3.43	0.35
GHN-JRM-0002-61	0.187	61.8	0.84	14.09	5.869	0.29	2.46	1.32	2.98	3.54	0.33
GHN-JRM-0002-62	0.079	60.1	0.83	13.76	6.698	0.35	2.38	1.39	2.74	3.43	0.35
GHN-KMD-0088	whole rock	64.4	0.49	14.19	3.810	0.16	1.51	1.13	2.92	3.80	0.21
GHN-KMD-0088-56	1.000	68.6	0.35	13.34	2.763	0.11	1.08	1.03	2.83	4.33	0.14
GHN-KMD-0088-57	0.750	66.4	0.46	14.19	3.599	0.16	1.47	0.98	3.25	4.10	0.19
GHN-KMD-0088-58	0.500	65.9	0.47	14.08	3.551	0.30	1.38	0.86	2.94	3.91	0.20
GHN-KMD-0088-61	0.187	65.6	0.49	14.14	3.709	0.17	1.58	1.05	2.82	3.89	0.21
GHN-KMD-0088-62	0.079	65.5	0.48	13.99	3.593	0.18	1.58	0.95	2.63	3.90	0.21
MIN-AAF-0001	whole rock	73.3	0.39	12.82	2.740	0.02	0.66	0.10	0.39	4.29	0.11
MIN-AAF-0001-56	1.000	71.7	0.44	13.30	2.054	0.03	0.85	0.16	1.29	5.76	0.15
MIN-AAF-0001-57	0.750	73.7	0.32	13.02	2.233	0.01	0.54	0.09	1.01	4.29	0.08
MIN-AAF-0001-58	0.500	73.4	0.42	13.40	2.133	0.02	0.71	0.21	0.63	4.39	0.09
MIN-AAF-0001-61	0.187	74.8	0.41	12.60	1.856	0.03	0.67	0.08	0.48	4.25	0.09
MIN-AAF-0001-62	0.079	73.8	0.38	12.67	2.353	0.02	0.61	0.10	0.45	4.28	0.10
MIN-AAF-0004	whole rock	71.9	0.38	13.14	2.900	0.02	0.62	0.09	0.45	4.39	0.12
MIN-AAF-0004-56	1.000	72.2	0.44	13.43	2.507	0.03	0.76	0.76	1.67	4.04	0.13
MIN-AAF-0004-57	0.750	71.1	0.56	13.57	2.696	0.03	0.79	0.34	1.14	4.39	0.15
MIN-AAF-0004-58	0.500	76.1	0.31	12.64	1.397	0.02	0.53	0.05	0.25	4.53	0.06
MIN-AAF-0004-61	0.187	74.2	0.41	12.74	2.017	0.02	0.68	0.08	0.43	4.27	0.08
MIN-AAF-0004-62	0.079	73.5	0.39	12.60	2.421	0.02	0.63	0.09	0.43	4.22	0.10
MIN-SAN-0002	whole rock	71.1	0.45	12.74	2.690	0.02	0.64	0.10	0.69	4.23	0.12
MIN-SAN-0002-57	0.750	72.6	0.46	13.12	2.092	0.03	0.70	0.13	0.83	4.50	0.11
MIN-SAN-0002-58	0.500	73.3	0.41	13.19	1.845	0.03	0.63	0.06	0.53	4.64	0.07
MIN-SAN-0002-61	0.187	73.3	0.38	12.65	1.903	0.02	0.62	0.09	0.51	4.18	0.08
MIN-SAN-0002-62	0.079	71.7	0.37	12.52	2.591	0.02	0.63	0.09	0.42	4.10	0.11
QPS-AAF-0001	whole rock	66.2	0.60	14.16	3.530	0.05	1.23	0.89	1.85	3.61	0.20
QPS-AAF-0001-56	1.000	69.4	0.63	14.72	2.924	0.03	1.00	0.44	2.00	3.18	0.36
QPS-AAF-0001-57	0.750	66.9	0.56	14.31	3.667	0.03	1.11	0.75	1.95	3.48	0.22
QPS-AAF-0001-58	0.500	66.5	0.56	14.02	3.716	0.03	1.18	0.89	1.37	3.62	0.21
QPS-AAF-0001-61	0.187	67.1	0.63	14.22	3.474	0.03	1.23	0.71	1.54	3.61	0.21
QPS-AAF-0001-62	0.079	66.0	0.63	14.31	3.786	0.04	1.27	0.87	1.45	3.68	0.21
QPS-AAF-0003	whole rock	63.1	0.59	14.53	4.360	0.05	1.57	1.25	1.88	3.71	0.24
QPS-AAF-0003-56	1.000	66.6	0.60	12.92	3.761	0.12	2.10	1.82	1.99	2.97	0.25

Sample	Size Fraction (inch)	SiO_2	TiO_2	Al_2O_3	FeOT	MnO	MgO	CaO	Na_2O	K_2O	P_2O_5
QPS-AAF-0003-57	0.750	64.8	0.56	14.28	4.137	0.06	1.49	1.32	2.69	3.62	0.24
QPS-AAF-0003-58	0.500	64.8	0.62	14.29	4.045	0.06	1.70	1.07	2.64	3.38	0.25
QPS-AAF-0003-61	0.187	64.8	0.59	14.18	4.011	0.05	1.53	1.12	2.22	3.61	0.22
QPS-AAF-0003-62	0.079	63.8	0.60	14.11	4.112	0.05	1.60	1.21	2.04	3.58	0.23
QPS-AAF-0005	whole rock	61.9	0.60	14.31	4.400	0.05	1.54	1.44	1.82	3.65	0.23
QPS-AAF-0005-56	1.000	65.4	0.57	15.18	4.021	0.05	1.05	0.58	4.26	3.56	0.22
QPS-AAF-0005-57	0.750	66.6	0.60	14.63	3.507	0.05	1.31	0.49	3.45	4.07	0.19
QPS-AAF-0005-58	0.500	64.0	0.61	14.37	3.963	0.05	1.53	1.15	2.54	3.96	0.22
QPS-AAF-0005-61	0.187	64.7	0.59	14.48	3.924	0.06	1.55	0.81	2.50	3.85	0.21
QPS-AAF-0005-62	0.079	64.1	0.60	14.48	3.998	0.06	1.71	0.96	2.20	3.71	0.22
QPS-AAF-0009		64	0.692	14.47	3.94	0.03	1.02	1.61	1.21	3.65	0.263
QPS-AAF-0009-56	1.000	63.0	0.71	15.75	4.306	0.07	2.01	2.32	2.23	3.72	0.31
QPS-AAF-0009-57	0.750	62.9	0.66	14.02	4.536	0.05	1.44	2.79	1.78	3.18	0.25
QPS-AAF-0009-58	0.500	64.1	0.72	15.05	3.989	0.05	1.37	1.71	1.39	3.91	0.26
QPS-AAF-0009-61	0.187	65.2	0.69	14.46	3.792	0.04	1.27	1.43	1.40	3.66	0.22
QPS-AAF-0009-62	0.079	63.7	0.69	14.35	4.074	0.03	1.13	1.68	1.12	3.69	0.23
QPS-SAN-0002	whole rock	67.7	0.50	13.66	3.060	0.02	0.93	0.68	1.24	3.71	0.17
QPS-SAN-0002-57	0.750	70.7	0.37	12.61	3.002	0.02	0.85	0.63	1.00	3.78	0.15
QPS-SAN-0002-58	0.500	71.4	0.44	13.12	2.216	0.02	0.82	0.63	1.21	3.53	0.15
QPS-SAN-0002-61	0.187	68.7	0.49	13.48	2.926	0.03	0.96	0.73	1.34	3.63	0.17
QPS-SAN-0002-62	0.079	64.0	0.51	13.42	4.371	0.03	1.08	1.04	1.15	3.61	0.23
SPR-SAN-0002		59.8	0.73	14.39	5.36	0.11	2.96	2.31	2.79	3.5	0.38
SPR-SAN-0002-57	0.750	60.6	0.78	15.06	5.165	0.10	3.16	2.40	3.08	3.30	0.32
SPR-SAN-0002-58	0.500	60.9	0.75	15.18	5.309	0.09	3.00	1.98	3.25	3.53	0.36
SPR-SAN-0002-61	0.187	61.6	0.73	14.43	4.826	0.09	2.89	2.19	3.04	3.62	0.34
SPR-SAN-0002-62	0.079	59.3	0.72	14.30	5.261	0.13	3.07	2.48	2.78	3.40	0.34

Sample	S	SO_4	C	LOI	Ni	Cr	Sc	V	Ba	Rb	Sr	Zr	Y
GHN-JRM-0001	2.01	1.12	0.07	8.81	30	57	9	74	832	134	136	163	25
GHN-JRM-0001-56	3.13	0.25	0.02	5.2	23	55	10	89	773	147	85	139	23
GHN-JRM-0001-57	2.43	0.34	0.02	5.09	13	46	8	73	795	120	146	147	24
GHN-JRM-0001-58	2.19	0.27	0.01	4.87	24	47	7	58	801	126	155	165	27
GHN-JRM-0001-61	2	0.57	0.02	6.55	20	50	8	65	860	138	138	171	27
GHN-JRM-0001-62	1.93	0.82	0.03	7.71	16	53	8	73	836	133	139	164	27
GHN-JRM-0002	0.14	0.34	0.06	4.66	49	87	11	106	1223	93	512	173	19
GHN-JRM-0002-56	0	0.13	0.03	2.96	48	81	8	98	1333	72	609	180	15
GHN-JRM-0002-57	0.09	0.22	0.02	4.04	40	81	9	100	1554	100	502	170	13
GHN-JRM-0002-58	0.08	0.11	0.02	3.9	40	85	9	96	1357	83	511	180	14
GHN-JRM-0002-61	0.07	0.16	0.01	4.25	40	83	9	100	1322	89	490	182	14
GHN-JRM-0002-62	0.02	0.38	0.02	5.53	41	83	10	99	1287	89	461	170	16
GHN-KMD-0088	0.41	0.04	5.14	5.14	31	47	6	60	1216	102	374	176	26
GHN-KMD-0088-56	0.84	0.32	0.06	3.87	13	30	5	41	776	124	293	229	43
GHN-KMD-0088-57	0.71	0.24	0.02	3.8	17	40	7	56	1049	101	365	202	32
GHN-KMD-0088-58	0.83	0.29	0.07	4.46	18	43	6	52	987	112	335	180	62
GHN-KMD-0088-61	0.52	0.37	0.02	4.58	19	47	7	61	1070	109	341	187	27
GHN-KMD-0088-62	0.34	0.36	0.02	4.69	20	44	7	61	1076	109	324	182	30
MIN-AAF-0001	0	0.38	0.23	4.27	0	24	4	46	591	149	92	229	36
MIN-AAF-0001-56	0.04	0.14	0.1	2.55	7	34	7	59	1034	160	135	259	42

Sample	S	SO_4	C	LOI	Ni	Cr	Sc	V	Ba	Rb	Sr	Zr	Y
MIN-AAF-0001-57	0.07	0.22	0.17	3.12	5	28	4	39	609	130	65	276	48
MIN-AAF-0001-58	0.02	0.21	0.1	3.25	7	27	5	48	544	146	98	231	35
MIN-AAF-0001-61	0.02	0.21	0.11	3.42	4	28	5	47	494	144	68	248	42
MIN-AAF-0001-62	0.01	0.33	0.16	3.95	5	25	4	40	579	141	93	241	38
MIN-AAF-0004	0.01	0.43	0.26	4.71	0	25	3	47	658	150	102	240	37
MIN-AAF-0004-56	0.02	0.09	0.1	2.92	5	17	6	53	720	122	223	238	33
MIN-AAF-0004-57	0.05	0.19	0.16	3.65	8	37	7	65	953	142	190	208	27
MIN-AAF-0004-58	0.02	0.14	0.1	3.15	3	17	3	32	510	148	48	267	47
MIN-AAF-0004-61	0.04	0.2	0.11	3.45	4	25	5	43	568	141	80	244	36
MIN-AAF-0004-62	0.04	0.32	0.13	4.11	5	24	5	43	626	139	105	237	38
MIN-SAN-0002	0	0.54	0.3	4.68	3	31	5	57	703	138	116	229	35
MIN-SAN-0002-57	0.04	0.17	0.1	3.59	0	34	6	52	890	143	105	241	34
MIN-SAN-0002-58	0.04	0.2	0.07	3.33	0	28	5	50	728	153	70	227	35
MIN-SAN-0002-61	0.03	0.23	0.09	3.74	0	25	5	42	577	133	114	240	40
MIN-SAN-0002-62	0	0.39	0.15	4.71	0	27	5	44	649	134	113	224	39
QPS-AAF-0001	0.11	0.55	0.09	5.27	11	66	9	83	1017	99	326	176	23
QPS-AAF-0001-56	0.31	0.18	0.04	3.77	15	63	10	86	1058	84	424	178	22
QPS-AAF-0001-57	0.17	0.57	0.05	4.8	19	64	9	76	877	94	349	184	31
QPS-AAF-0001-58	0.12	0.74	0.04	5.84	16	62	10	84	883	102	275	179	24
QPS-AAF-0001-61	0.1	0.61	0.05	5.43	17	70	10	86	954	103	312	175	21
QPS-AAF-0001-62	0.04	0.72	0.06	5.81	18	71	10	88	927	104	309	177	21
QPS-AAF-0003	0.06	0.91	0.03	6.74	20	63	9	88	1416	117	362	168	20
QPS-AAF-0003-56	1.07	0.43	0.16	5.06	42	69	11	84	930	92	311	151	24
QPS-AAF-0003-57	0.17	0.54	0.06	4.81	30	57	9	76	1100	110	734	167	21
QPS-AAF-0003-58	0.22	0.61	0.06	5.32	31	70	9	82	1227	102	384	164	21
QPS-AAF-0003-61	0.32	0.59	0.04	4.95	30	66	9	80	1070	106	379	165	20
QPS-AAF-0003-62	0.3	0.76	0.04	6.05	30	67	9	82	1094	107	377	163	20
QPS-AAF-0005	0.02	1.17	0.03	8.03	17	61	10	86	1086	116	371	169	18
QPS-AAF-0005-56	0.25	0.22	0.03	3.2	23	52	8	72	1156	99	571	175	18
QPS-AAF-0005-57	0.12	0.26	0.02	3.47	24	59	9	83	1396	118	461	173	14
QPS-AAF-0005-58	0.09	0.64	0.02	5.47	23	64	9	83	1188	120	385	171	17
QPS-AAF-0005-61	0.06	0.59	0.03	5.37	24	62	9	82	1171	115	384	172	18
QPS-AAF-0005-62	0.06	0.71	0.05	6.52	24	64	10	88	1186	112	370	170	19
QPS-AAF-0009	0.18	1.18	0.03	6.93	11	68	10	97	933	103	380	170	18
QPS-AAF-0009-56	0.22	0.38	0.06	3.7	33	81	12	101	1264	87	530	168	17
QPS-AAF-0009-57	0.62	1.03	0.02	6.1	24	70	10	93	1028	83	338	151	14
QPS-AAF-0009-58	0.23	0.68	0.02	5.05	20	73	11	107	1015	101	319	165	16
QPS-AAF-0009-61	0.2	0.73	0.02	5.44	17	66	11	96	1024	96	345	165	17
QPS-AAF-0009-62	0.17	1.08	0.03	6.57	15	69	11	102	1014	100	346	164	17
QPS-SAN-0002	0	0.97	0.04	5.13	8	48	8	69	724	109	285	200	29
QPS-SAN-0002-57	0.08	0.48	0.02	4.69	4	37	5	44	947	111	210	230	44
QPS-SAN-0002-58	0.31	0.39	0.02	4.34	7	44	5	53	730	100	226	208	38
QPS-SAN-0002-61	0.15	0.63	0.05	5.48	6	50	8	64	790	104	299	193	31
QPS-SAN-0002-62	0.05	1.17	0.04	7.42	7	58	8	71	799	108	335	185	29
SPR-SAN-0002	0.18	0.46	0.05	4.22	62.8	106	13.8	122	1075	112.6	725	166.5	20.5
SPR-SAN-0002-57	1.28	0.08	0.07	3.93	58	121	13	123	1206	119	898	176	20
SPR-SAN-0002-58	0.79	0.1	0.03	3.31	64	106	13	115	1150	113	676	181	20
SPR-SAN-0002-61	0.49	0.19	0.06	3.9	55	99	12	107	1182	113	665	172	20
SPR-SAN-0002-62	0.23	0.51	0.15	5.7	62	106	13	110	1084	113	746	166	19

Sample	Nb	Ga	Cu	Zn	Pb	La	Ce	Th	Nd	U	F
GHN-JRM-0001	16	21	172	92	153	49	96	11	40.3	5	1646

Sample	Nb	Ga	Cu	Zn	Pb	La	Ce	Th	Nd	U	F
GHN-JRM-0001-56	16	19	78	52	62	36	75	9	30.5	3.7	
GHN-JRM-0001-57	16	19	73	138	48	34	65	9	28.2	3.7	
GHN-JRM-0001-58	17	20	124	86	57	34	72	10	29.7	4.6	
GHN-JRM-0001-61	17	21	139	86	61	43	90	10	37.4	3.7	
GHN-JRM-0001-62	16	20	165	113	84	46	92	10	38.6	4.8	
GHN-JRM-0002	12	21	88	295	131	45	102	7	46	1.1	1047
GHN-JRM-0002-56	13	17	28	244	35	35	83	7	36.1	2.6	
GHN-JRM-0002-57	12	19	51	221	37	36	82	8	37.7	3.1	
GHN-JRM-0002-58	12	18	51	240	56	30	69	7	32.9	3.5	
GHN-JRM-0002-61	13	18	61	266	84	36	79	7	37.3	1.9	
GHN-JRM-0002-62	12	19	94	301	137	39	92	8	38.2	2.8	
GHN-KMD-0088	13	20	40	221	60	41	102	7	53.8	4	1015
GHN-KMD-0088-56	21	19	37	127	41	51	125	12	61.1	4.2	
GHN-KMD-0088-57	17	18	35	252	95	46	100	11	48.8	4.9	
GHN-KMD-0088-58	16	20	28	359	47	83	193	11	102	4.5	
GHN-KMD-0088-61	16	19	34	214	60	43	106	10	51.6	4.2	
GHN-KMD-0088-62	16	20	32	223	167	49	121	10	59.1	4.4	
MIN-AAF-0001	25	22	18	20	93	54	102	13	40	3	1284
MIN-AAF-0001-56	24	21	15	27	54	46	87	11	36.1	3.9	747
MIN-AAF-0001-57	29	24	27	19	176	56	105	12	47.1	4	924
MIN-AAF-0001-58	28	24	12	17	51	47	96	12	36.2	3.5	1098
MIN-AAF-0001-61	27	22	16	22	83	54	111	12	43.1	4	1098
MIN-AAF-0001-62	27	20	16	20	91	53	102	13	40.2	4.7	1057
MIN-AAF-0004	26	23	23	21			124	16		2	1258
MIN-AAF-0004-56	23	21	13	27	39	38	76	11	28	3.3	913
MIN-AAF-0004-57	21	19	18	32	56	45	82	10	31.1	3.9	1044
MIN-AAF-0004-58	29	22	12	18	70	43	89	12	34.5	5.1	1071
MIN-AAF-0004-61	25	21	21	21	74	53	97	11	37.2	4.2	1089
MIN-AAF-0004-62	26	21	19	21	92	49	95	12	36.7	3	958
MIN-SAN-0002	25	22	25	19			88	13		3.9	1092
MIN-SAN-0002-57	24	21	45	22	117	41	80	13	34.5	3.3	
MIN-SAN-0002-58	23	21	14	16	62	45	90	13	36.4	4.4	
MIN-SAN-0002-61	26	22	14	19	59	50	98	12	37.7	3.4	
MIN-SAN-0002-62	25	21	19	19	92	51	98	13	37.5	3.9	
QPS-AAF-0001	15	21	39	64			47	11		3.8	
QPS-AAF-0001-56	14	20	44	39	25	34	69	9	28.5	3	801
QPS-AAF-0001-57	18	21	25	54	40	40	73	10	32.4	2	907
QPS-AAF-0001-58	16	20	31	44	44	36	75	9	29.2	4.9	1829
QPS-AAF-0001-61	15	21	35	46	44	34	67	7	30.5	4.4	982
QPS-AAF-0001-62	14	19	37	50	59	38	69	9	29.1	2.4	1220
QPS-AAF-0003	13	21	44	82			55	11		3	1291
QPS-AAF-0003-56	10	16	64	108	52	29	66	6	33.1	1.6	3373
QPS-AAF-0003-57	12	19	50	91	33	34	65	9	31.5	4	2354
QPS-AAF-0003-58	12	20	41	87	44	35	65	8	30.7	1.9	1090
QPS-AAF-0003-61	12	20	51	85	40	33	65	8	29.8	2.7	2145
QPS-AAF-0003-62	13	19	46	85	46	33	61	7	27.5	2.6	1453
QPS-AAF-0005	12	20	43	73			58	10		2	1164
QPS-AAF-0005-56	12	16	28	69	28	25	48	11	24.3	2.1	599
QPS-AAF-0005-57	11	18	26	63	30	24	43	9	21	1.6	745
QPS-AAF-0005-58	14	19	36	76	48	29	58	9	24.6	2.3	1801
QPS-AAF-0005-61	12	20	39	77	54	30	57	8	22.8	0.6	937
QPS-AAF-0005-62	14	19	41	81	54	35	60	8	24.6	0.9	997

Sample	Nb	Ga	Cu	Zn	Pb	La	Ce	Th	Nd	U	F
QPS-AAF-0009	11.5	19	29	29	40	37	67	9	29	3	940
QPS-AAF-0009-56	11	20	41	55	26	39	77	8	32.1	1.1	872
QPS-AAF-0009-57	10	17	19	45	71	32	64	6	28.6	3.5	765
QPS-AAF-0009-58	11	20	25	37	24	38	69	6	29.1	2.7	918
QPS-AAF-0009-61	10	20	31	35	26	36	67	5	27.8	3.3	961
QPS-AAF-0009-62	11	19	30	31	36	34	67	6	27.3	3.7	885
QPS-SAN-0002	19	23	34	34			33	11		5.1	1070
QPS-SAN-0002-57	28	22	32	31	47	66	108	13	37.4	5.1	
QPS-SAN-0002-58	23	21	27	31	24	56	105	11	41.3	4.3	
QPS-SAN-0002-61	19	21	30	37	33	52	93	11	29	5	
QPS-SAN-0002-62	18	22	38	42	50	42	76	10	29.8	3.7	
SPR-SAN-0002	10.9	18.7	139	47.9	20.7	46.6	89.3	8	37.5	3	2498
SPR-SAN-0002-57	11	19	132	42	8	43	83	9	36	3.6	
SPR-SAN-0002-58	12	19	147	49	20	42	84	9	36	2.1	
SPR-SAN-0002-61	12	18	123	62	24	44	87	9	38	2.7	
SPR-SAN-0002-62	10	18	150	64	30	50	92	9	38.9	4.1	

TABLE 1-4. Mineral composition of samples and different particle size fractions in weight percent.

Sample	Quartz	K-feldspar	Plagioclase	Epidote	Calcite	Pyrite	Fe Oxides	Rutile
GHN-JRM-0001	35	7	15	0.01	0.4	3	0.01	0.5
GHN-JRM-0001-56	33	21	12	0.01	0.09	5	0.01	0.5
GHN-JRM-0001-57	32	18	21	0.01	0.01	4	0.7	0.5
GHN-JRM-0001-58	34	21	14	0.01	0.09	4	1	0.5
GHN-JRM-0001-61	35	18	12	0.01	0.09	3	0.3	0.5
GHN-JRM-0001-62	35	14	13	0.01	0.09	3	0.2	0.5
GHN-JRM-0002	26	18	19	0.3	0.6	0.3	7	0.5
GHN-JRM-0002-56	24	24	26	4	0.3	0.01	4	0.6
GHN-JRM-0002-57	26	25	18	2	0.2	0.2	4	0.7
GHN-JRM-0002-58	26	22	22	2	0.2	0.09	5	0.7
GHN-JRM-0002-61	27	22	19	2	0.09	0.09	6	0.6
GHN-JRM-0002-62	27	20	18	0.01	0.09	0.01	7	0.5
GHN-KMD-0088	29	23	19	0.01	0.01	0.9	3	0.5
GHN-KMD-0088-56	33	30	16	0.01	0.4	1	2	0.3
GHN-KMD-0088-57	28	28	20	0.01	0.2	1	3	0.4
GHN-KMD-0088-58	31	23	19	0.01	0.6	1	2	0.4
GHN-KMD-0088-61	30	24	18	0.01	0	0.9	3	0.4
GHN-KMD-0088-62	31	23	17	0.01	0	0.6	3	0.4
MIN-AAF-0001	47	15	0	0.01	0.1	0.01	2	0.3
MIN-AAF-0001-56	38	36	2	0.01	0.6	0.1	1	0.4
MIN-AAF-0001-57	45	19	4	0.01	0.8	0.09	2	0.3
MIN-AAF-0001-58	45	18	0.6	0.01	0.7	0.01	2	0.4
MIN-AAF-0001-61	47	21	0.01	0.01	0.2	0.01	2	0.3
MIN-AAF-0001-62	48	16	0.01	0.01	0.8	0.01	2	0.3

Sample	Quartz	K-feldspar	Plagioclase	Epidote	Calcite	Pyrite	Fe Oxides	Rutile
MIN-AAF-0004	43	22	0.01		0.4	0.01	3	0.2
MIN-AAF-0004-56	40	22	8		0.9	0.01	3	0.3
MIN-AAF-0004-57	41	21	4		1	0.09	2	0.5
MIN-AAF-0004-58	50	15	1		0.5	0.01	0.9	0.3
MIN-AAF-0004-61	47	18	0.01		0.6	0.09	1	0.4
MIN-AAF-0004-62	47	15	0.01		0.7	0.09	2	0.3
MIN-SAN-0002	48	4	10		0.2		0.8	0.4
MIN-SAN-0002-57	48	11	6		0.6	0.09	2	0.4
MIN-SAN-0002-58	49	14	0.8		0.4	0.09	1	0.4
MIN-SAN-0002-61	51	10	2		0.5	0.09	1	0.3
MIN-SAN-0002-62	47	13	0.2		0.2	0.01	2	0.3
QPS-AAF-0001	38	12	13	0.01	0.7	0.2	2	0.5
QPS-AAF-0001-56	39	11	15	0.01	0.01	0.6	3	0.6
QPS-AAF-0001-57	38	10	15	0.01	0.3	0.3	3	0.5
QPS-AAF-0001-58	40	8	10	0.01	0.2	0.2	2	0.5
QPS-AAF-0001-61	40	10	11	0.01	0.09	0.2	2	0.6
QPS-AAF-0001-62	39	8	11	0.01	0.4	0.09	3	0.6
QPS-AAF-0003	34	10	14		0.1	0.1	3	0.5
QPS-AAF-0003-56	38	14	13	0.01	1	2	2	0.6
QPS-AAF-0003-57	31	19	18	0.01	0.4	0.3	4	0.4
QPS-AAF-0003-58	33	13	19	0.01	0.4	0.4	3	0.5
QPS-AAF-0003-61	34	15	15	0.01	0.2	0.6	3	0.5
QPS-AAF-0003-62	34	12	15	0.01	0.2	0.6	3	0.5
QPS-AAF-0005	34	6	14	0.01	0.09		3	0.5
QPS-AAF-0005-56	25	22	30	0.01	0.09	0.5	4	0.4
QPS-AAF-0005-57	29	25	23	0.01	0	0.2	3	0.5
QPS-AAF-0005-58	30	19	17	0.01	0.01	0.2	3	0.5
QPS-AAF-0005-61	32	16	17	0.01	0.09	0.09	3	0.5
QPS-AAF-0005-62	33	12	16	0.01	0.3	0.09	3	0.5
QPS-AAF-0009	35	17	6	0.01	0.3	0.3	3	0.6
QPS-AAF-0009-56	27	19	14	3	0.5	0.4	3	0.6
QPS-AAF-0009-57	33	13	12	0.01	0.01	1	4	0.4
QPS-AAF-0009-58	32	16	8	0.01	0.01	0.4	4	0.5
QPS-AAF-0009-61	36	12	9	0.01	0.01	0.4	3	0.5
QPS-AAF-0009-62	37	7	8	0.01	0.09	0.3	3	0.5
QPS-SAN-0002	42	4	10		0.2		0.8	0.4
QPS-SAN-0002-57	44	14	5	0.01	0.09	0.09	2	0.3
QPS-SAN-0002-58	44	13	7	0.01	0.09	0.6	1	0.4
QPS-SAN-0002-61	42	9	9	0.01	0.3	0.3	1	0.5
QPS-SAN-0002-62	41	1	10	0.01	0.2	0.09	2	0.4
SPR-SAN-0002	25	21	18	2	0.5	0.3	4	0.6
SPR-SAN-0002-57	24	21	20	7	0.6	2	0.6	0.7
SPR-SAN-0002-58	23	23	21	5	0.2	1	2	0.6
SPR-SAN-0002-61	25	24	19	5	0.5	0.8	2	0.7
SPR-SAN-0002-62	25	20	18	0.8	1	0.4	4	0.5

Sample	Gypsum	Apatite	Kaolinite	Chlorite	Illite	Smectite	Jarosite	Zircon

Sample	Gypsum	Apatite	Kaolinite	Chlorite	Illite	Smectite	Jarosite	Zircon
GHN-JRM-0001	1	0.2	0.9	3	27	2	4	0.03
GHN-JRM-0001-56	0.3	0.4	0.9	3	21	2	1	0.03
GHN-JRM-0001-57	0.5	0.3	0.9	3	16	2	1	0.03
GHN-JRM-0001-58	0.4	0.4	0.9	3	17	2	0.9	0.03
GHN-JRM-0001-61	0.7	0.3	0.9	3	22	2	2	0.03
GHN-JRM-0001-62	1	0.2	0.9	3	24	2	3	0.03
GHN-JRM-0002	1.6	0.9		6	16	4	0.01	0.03
GHN-JRM-0002-56	0.6	0.8	0	6	6	4	0.01	0.03
GHN-JRM-0002-57	1	0.7	0	7	12	4	0.01	0.03
GHN-JRM-0002-58	1	0.8	0	6	11	4	0.01	0.03
GHN-JRM-0002-61	0.8	0.8	0	6	12	4	0.01	0.03
GHN-JRM-0002-62	2	0.7	0	6	15	4	0.01	0.03
GHN-KMD-0088	2	0.4	2	4	14	2	0.01	0.03
GHN-KMD-0088-56	1.09	0.2	2	3	9	2	0.01	0.03
GHN-KMD-0088-57	1.07	0.5	2	4	10	2	0	0.03
GHN-KMD-0088-58	0.96	0.3	2	4	14	2	0.5	0.03
GHN-KMD-0088-61	2.1	0.3	2	4	14	2	0	0.03
GHN-KMD-0088-62	1.09	0.3	2	4	15	2	0.3	0.03
MIN-AAF-0001	0.1	0.1	2	2	29	1	2	0.04
MIN-AAF-0001-56	0.01	0.01	2	2	16	1	0.7	0.04
MIN-AAF-0001-57	0.01	0.01	2	1	24	0.9	1	0.04
MIN-AAF-0001-58	0.01	0.01	2	2	28	0.9	1	0.04
MIN-AAF-0001-61	0.01	0.09	2	2	24	0.9	1	0.04
MIN-AAF-0001-62	0.01	0.01	0.9	2	28	0.9	2	0.04
MIN-AAF-0004	0.01	0.01	2	1	25	0.9	2	0.04
MIN-AAF-0004-56	0.4	0.3	2	2	20	1		0.04
MIN-AAF-0004-57	0.01	0.01	2	2	24	0.9	1	0.04
MIN-AAF-0004-58	0	0.01	2	1	27	0.9	0.7	0.04
MIN-AAF-0004-61	0	0.01	2	2	27	0.9	1	0.04
MIN-AAF-0004-62	0.01	0.01	2	2	28	0.9	2	0.04
MIN-SAN-0002	1	0.2	1	3	31	3	4	0.04
MIN-SAN-0002-57	0.01	0.01	3	2	26	0.9	0.9	0.04
MIN-SAN-0002-58	0.01	0.01	3	2	27	0.9	1	0.04
MIN-SAN-0002-61	0.01	0.01	3	2	28	0.9	1	0.04
MIN-SAN-0002-62	0.01	0.09	3	2	29	0.9	2	0.04
QPS-AAF-0001	0.9	0.4		3	27		2	0.03
QPS-AAF-0001-56	0.4	0.6		3	27		0.6	0.03
QPS-AAF-0001-57	0.9	0.4		3	27		2	0.03
QPS-AAF-0001-58	1	0.4		3	31		3	0.03
QPS-AAF-0001-61	0.9	0.4		3	30		2	0.03
QPS-AAF-0001-62	1	0.4		3	31		3	0.03
QPS-AAF-0003	2	0.4	1	4	28	1	2	0.03
QPS-AAF-0003-56	2	0.5	0.9	6	19	0.9		0.03
QPS-AAF-0003-57	2	0.4	0.9	4	18	0.9	0.7	0.03
QPS-AAF-0003-58	1	0.4	0.9	5	21	0.9	2	0.03

Sample	Gypsum	Apatite	Kaolinite	Chlorite	Illite	Smectite	Jarosite	Zircon
QPS-AAF-0003-61	2	0.4	0.9	4	22	0.9	1	0.03
QPS-AAF-0003-62	2	0.4	0.9	4	25	0.9	2	0.03
QPS-AAF-0005	2	0.4	3	4	29	0.9	3	0.03
QPS-AAF-0005-56	0.7	0.3	3	2	10	0.9	0.4	0.03
QPS-AAF-0005-57	0.6	0.3	3	3	11	0.9	0.7	0.03
QPS-AAF-0005-58	2	0.4	3	4	19	0.9	1	0.03
QPS-AAF-0005-61	1	0.4	3	4	20	0.9	2	0.03
QPS-AAF-0005-62	1	0.4	3	4	24	0.9	2	0.03
QPS-AAF-0009	0.9	0.7	1	3	28	1	3	0.03
QPS-AAF-0009-56	2	0.7	0.9	5	22	2		0.03
QPS-AAF-0009-57	5	0.4	2	4	25	0.9		0.03
QPS-AAF-0009-58	3	0.4	2	3	29	0.9	0.3	0.03
QPS-AAF-0009-61	2	0.4	2	3	29	0.9	1	0.03
QPS-AAF-0009-62	3	0.4	0.9	3	34	0.9	2	0.03
QPS-SAN-0002	1	0.2	1	3	31	3	4	0.04
QPS-SAN-0002-57	0.8	0.3	0.9	2	25	3	2	0.04
QPS-SAN-0002-58	0.8	0.3	0.9	2	26	3	1	0.04
QPS-SAN-0002-61	0.8	0.3	0.9	2	28	3	2	0.04
QPS-SAN-0002-62	1	0.4	0.9	3	33	3	4	0.04
SPR-SAN-0002	2	0.9	1	8	14	3		0.03
SPR-SAN-0002-57	0.4	0.7	0.9	8	11	3		0.03
SPR-SAN-0002-58	0.5	0.8	0.9	8	11	3		0.03
SPR-SAN-0002-61	0.9	0.8	0.9	8	10	3		0.03
SPR-SAN-0002-62	2	0.8	0.9	8	15	3		0.03